Electrochemical Nanoimprinting with Solid-State Superionic Stamps

Keng H. Hsu, Peter L. Schultz, Placid M. Ferreira, and Nicholas X. Fang*

Department of Mechanical Science & Engineering,
University of Illinois at Urbana–Champaign, Illinois 61801

ABSTRACT

This letter presents a solid-state electrochemical nanoimprint process for direct patterning of metallic nanostructures. It uses a patterned solid electrolyte or superionic conductor (such as silver sulfide) as a stamp and etches a metallic film by an electrochemical reaction. Our preliminary experiments demonstrate repeatable and high-fidelity pattern transfer with features down to 50 nm on silver films of thicknesses ranging from 50 to 500 nm. As the process is conducted in an ambient environment and does not involve the use of liquids, it displays potential for single-step, high-throughput, large-area manufacturing of metallic nanostructures. The use of superionic conductors in manufacturing opens up a new and potentially energy-efficient approach to nanopatterning and fabrication. It offers a highly competitive approach, both as a stand-alone process and as a complement of other nanofabrication techniques, to fabricating chemical sensors, photonic and plasmonic structures, and electronic interconnects.

Patterning nanoscale metallic features is an integral part of a wide variety of fabrication applications including nano-electronic, photonic, and nanoelectromechanical devices as well as nanoscale chemical sensors and transducers.[1,2] However, the common practice for generating metallic patterns has relied on an indirect approach: nanoscale patterns are first created on photoresist by optical lithography or by mechanical imprinting[3–5] and followed by metal deposition and the subsequent lift-off or etching processes. The damascene process pursued by the semiconductor industry, for instance, deposits the copper interconnects electrochemically into the trenches of patterned dielectrics and uses chemical mechanical polishing to remove excess metal in an expensive, complex, multistep process that requires stringent process environment control and very costly equipment. An alternative method, electrochemical micromachining (ECM), has been proposed to directly produce submicron metallic features.[6,7] However, significant limitations on lateral extension of the features are associated with electrochemical machining due to a considerable diffusion length of the reacting species. Accelerated etching at sharp edges and corners also leads to low geometrical fidelity in the pattern transferred from the electrochemical tool to the substrate surface.[6] In addition, the use of liquids might contaminate both the tool and the substrate.

In this letter, we address the above issues by introducing a solid-state electrochemical imprinting process that directly creates high-resolution metallic nanopatterns in a single step. The proposed process, which we have named solid-state superionic stamping (or S4), is schematically presented in Figure 1. At the core of this process is a solid electrolyte or superionic conductor[8] that is widely used in battery and fuel cells due to its excellent ionic conductivity at room and relatively low temperatures. A stamp made of a superionic conductor with a mobile cation (silver sulfide, for example, in which the silver ions are mobile) is pre-patterned with fine features and brought into contact with the metallic substrate to be patterned. On the application of an electrical bias with the substrate as an anode and a metallic electrode at the back of the stamp as a cathode, a solid-state electrochemical reaction takes place at the contact points of the interface. At the anode–electrolyte interface, an appreciable potential drop causes the oxidation of silver atoms on the substrate and produces mobile silver ions. These mobilized ions migrate across the interface and through the interstitial channels and defect network in the lattice of the superionic conductor toward the cathode until they recombine with electrons. The anodic dissolution progressively removes a metallic layer of the substrate at the contact area with the stamp. Assisted by a nominal pressure to maintain electrical contact, the stamp progresses into the substrate, generating a shape in the silver substrate complementary to the pre-patterned features on it. The advantage of using solid-state superionic conductors is that mass transport is restricted to the physical contact between the patterned electrolyte and the substrate (the anode), making it an ideal tool for nanoscale pattern transfer with high fidelity.

Our method is clearly distinguished from scanning probe-based electrochemical patterning methods in which the high
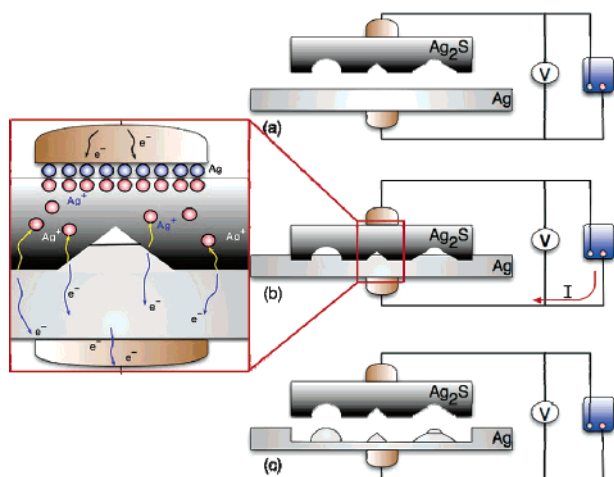

Figure 1. Schematic of the solid-state superionic stamping process. A stamp made of a solid ionic conductor is brought into contact with the workpiece or substrate to be patterned. A biasing electrical potential dissolves the metal at the workpiece(anode)−stamp interface. (a) To initiate solid-state ionic stamping, a prepatterned solid electrolyte (silver sulfide in our work) backed with an inert metal is connected to a potentiostat as the counter electrode (cathode), and the metal substrate to be patterned is the anode. (b) Pre-patterned solid electrolyte stamp is placed in contact with the metal workpiece or substrate and, with an applied voltage bias and nominal force, electrochemical etching takes place at the contact areas, progressively dissolving metal into the solid ionic stamp and engraving the workpiece. (c) Electrochemical imprinting is completed, resulting in a pattern on the metal substrate complementary to that on the solid electrolyte stamp.

spatial resolution stems from limited diffusion of the electrolyte ions[9] or geometrically confined liquid electrolyte volume.[10] The mobility of ions in an array of solid electrolytes such as Ag_2S and $RbAg_4I_5$ has been exploited to create nanostructures in "direct write" like processes. Subhundred nanometer line and dot patterns have been written using scanning probe microscopy.[11,12] These techniques use an electrical potential applied across a scanning probe and a solid electrolyte substrate surface to induce the migration of metal ions from within the substrate to the vicinity of the probe to form metallic clusters to create lines or dots on the electrolyte surface.[13] The practicality of this direct pattern writing as a manufacturing process is limited because of low throughput, difficulties in dimensional control of the structures formed, and processing parameters (the stand-off distance of the probe must be precisely regulated and its travel speed must be coordinated to the growth of the structure). Most importantly, the metal structures are embedded in the electrolyte surface layer, making their subsequent use in many applications difficult.

In this letter, we validate the concept of the S4 process through the use of silver sulfide as the solid-state superionic stamp for electrochemically imprinting silver nanoscale features, as shown in Figure 2. First, to prepare a silver sulfide stamp, we started with synthesizing a dense silver sulfide pellet in an improvised furnace with programmable temperature control. Sulfur powder with 99.999% purity (from Fisher Scientific Co.) was hand-pressed into a pellet of 3 mm in diameter and inserted into a glass tube (3 mm
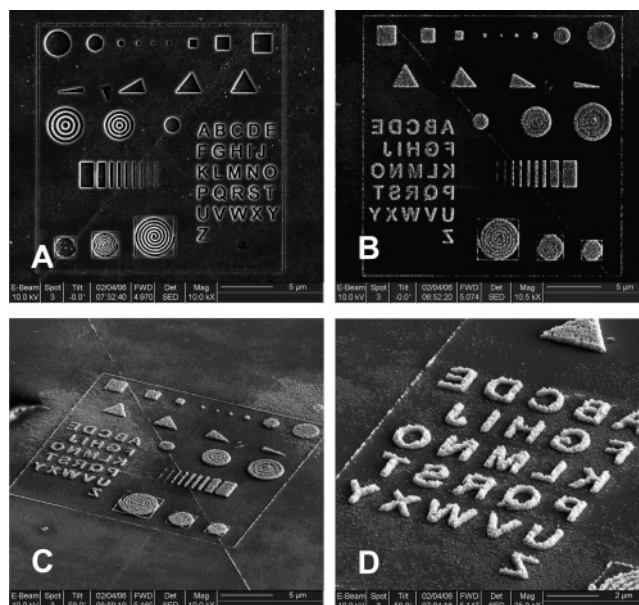
Figure 2. SEM images illustrating silver patterning with the S4 process. (a) FIB-patterned Ag_2S stamp with an array of geometric patterns and letters. The radius of the circles range from 2.4 μm to 200 nm; the squares are patterned with a range of width from 300 nm to 1.7 μm; the triangles are patterned with varying angles from 15° to 60° with 15° steps, and the radius of the acute corner is as small as 50 nm. Each of the concentric rings is made with uniform pitch, from left to right, the pitch measures 500, 390, and 240 nm, respectively. The rectangles are patterned with a width varying from 60 nm to 1.3 μm. To form the letters, the line width is set to be 200 nm and the depth is nearly 300 nm. (b) Solid-state etching results on a 250 nm thick evaporated silver film with 10 nm seed Cr layer on top of a glass substrate, showing a complementary nanopattern to that on the stamp. (c) Perspective view of the generated pattern. (d) Close-up view of the alphabet with 200 nm line width, showing an aspect ratio better than 1.

internal diameter) with a silver pellet (from Kurt J. Lesker Co.). The two were then held together with a small constant force (required for a dense silver sulfide pellet) provided by a spring. The assembly was placed in the furnace at 400 °C for 10 h to allow formation and annealing of silver sulfide. The silver sulfide pellets created in this manner were characterized with X-ray diffraction (Rigaku D-Max system with a scanning range (2-θ) from 0 to 60° and a scan rate of 0.8° per min) and compared with standard peaks for the powder form β-silver sulfide. Characterization of a number of pellets confirmed the composition of the silver sulfide pellets and the consistent output of the above process. The synthesized silver pellets were machined to a conical tip at one end. This end was planarized to produce a flat mesa of 300 μm in diameter for stamping. The patterns on the stamp, such as those shown in Figure 2A, were produced by focused ion-beam milling (FEI Dual-Beam DB-235) with a 50 pA aperture at a milling rate of about 50 nm/min. The deepest trench on the stamp in Figure 2A was about 250 nm. We also demonstrated direct embossing of the silver sulfide stamps against silicon molds.

For different patterning experiments, a number of silver substrates were prepared by electron beam evaporation of silver onto a 300 μm thick glass cover slip cleaned using

RCA1 solution. The silver films were deposited over a 10 nm Cr seed layer at a chamber pressure of 5×10^{-6} Torr and a stable rate of 0.1 nm/s. To perform stamping, the glass substrate with the silver film was then mounted on a glass window and a single-axis microactuator was used to feed the stamp down to the substrate. The stamp was attached to this assembly via an elastomer that provides 48 MPa of pressure at 20% compressive strain uniformly across the actual contact area between the electrode and the silver substrate. This nominal pressure (well below the yield stress of silver sulfide) ensured a consistent contact between the stamp and the substrate during the progress of electrochemical imprinting.

The electrical potential for electrochemical imprinting is controlled by a digital potentiostat (Gamry Instrument model Reference 600) with a blocking electrode attached to the stamp as the cathode and the silver substrate being patterned as the anode. The process was performed in the chrono-amperometry mode of the potentiostat in which the potential between anode and cathode was kept constant and the current was monitored. To produce the results shown in Figure 2B, electrochemical imprinting was performed with a driving potential of 0.8 V on a 250 nm thick silver film. Close-up views in the bottom panels confirm that all designed geometrical features with dimensions greater than 80 nm were successfully transferred with dimensional deviations from the stamp being less than 10 nm. The lateral resolution achieved is 100 nm for line width (as observed in the line pattern) and 80 nm for line spacing (in the concentric-ring pattern).

A remarkable feature of the S4 process, in contrast to the liquid-based electrochemical etching, is the capability of reproducing acute angles. As seen in parts B and C of Figure 2, even the triangle with a 15° angle was transferred with fine details at the tip (radius of curvature of 50 nm). This unique capability is essential for plasmonic devices and sensors that require a sharp geometric singularity for effective and controllable enhancement of an optical near field, such as surface enhanced raman scattering (SERS). In addition, solid-state electrochemical imprinting offers excellent pattern transfer fidelity. Our measurements indicate that the mismatch between the feature size on the stamp and that of the formed complementary pattern on silver substrate is less than 10 nm, only about one-tenth of what can be achieved in liquid-state electrochemical machining, even with nanosecond pulse methods to constraint field diffusion.[7] Improving the pattern transfer fidelity through optimization of the process parameters such as the applied bias and contact pressure is one of our ongoing efforts.

One can also observe in Figure 2B that the surface and edges of the transferred silver pattern appear to be relatively rough as compared to the exposed Cr surface. This can be attributed to an insufficient relief depth on the silver sulfide stamp made by FIB patterning, resulting in undesired contact between the relieved stamp surfaces; the resulting dissolution at these undesired contact surfaces coupled with the use of relatively high electrical potential (0.8 V) increases the rate of nucleation and growth of pores on the metal surface. In

addition, during intermediate etch steps and after extended etching, it is also typical to observe silver clusters tens of nanometers in diameter and height dispersed on the Cr surface, even though such features are not noticeable on the polished stamp surface. These are thought to have originated from the nucleation-growth-of-pore nature[14] of the silver electrode dissolution. A detailed study of the mechanical and chemical conditions of the contacts at the stamp−metal interface and their impact on the patterning will be addressed in our future work.

To verify the electrochemical activity, we also performed a set of linear-anodic-sweep experiments between the stamp and 250 nm thick silver substrate (the anode) with a scan range from 0 to 0.5 V at a speed of 20 mV/s (Figure 3A). A distinct peak in total current is observed between 0.1 and 0.2 V as the applied bias is increased. This peak can be associated with the anodic dissolution of silver by breaking the space charge layer at the silver−electrolyte interface and the acceleration of this process with increasing anodic bias. Upon further increase in anodic bias beyond this point, however, the total current does not follow the same increasing trend but instead falls down rapidly. This behavior can be rationalized by considering the switching of the anodic dissolution from charge-transfer control to diffusion control: the silver ion accumulation at the vicinity of the interface resulting from the finite rate of migration of silver ions in the stamp gives rise to a concentration overpotential that counteracts with the applied potential, decreasing the dissolution rate. As the anodic bias keeps increasing, the concentration overpotential resulting from the increased silver ion flux also increases and blocks the ionic flux from the dissolving interface, causing a drop of current density until about 0.26 V applied bias. This characteristic hump curve in the forward voltage sweep is clearly distinguished from the anodic sweeping curve measured from a blocking electrode made of carbon, which simply indicates the Ohmic response of electronic conductivity of Ag_2S (a typical n-type semiconductor) in the same potential range. The difference between the two curves in Figure 3A clearly indicates the ionic activity between the silver substrate and the stamp.

We present in Figure 3B the total current evolution during the electrochemical etching processes obtained when using new or unused Ag_2S stamps at different voltages to etch a 250 nm thick silver film. Currents for the higher voltage levels (0.4−0.8 V) follow a similar trend: they ramp up to their highest values with activation of the electrochemical reaction and slope down to lower values in the second stage as polarization of the stamp increases. The current then decreases sharply as a result of the depletion of silver at the anode and stabilizes with a low but nonzero value (which corresponds to the electronic conduction, as Ag_2S is a mixed conductor), indicating a completion of the process. This depletion of silver is verified by observations from the back side of the optically transparent glass substrate. Except for 0.2 V bias, which did not etch through the thickness of the film, we integrated the areas under different current curves and found the total charge transferred (about 3.9×10^{-3} coulomb) is nearly equal for the different applied biases. This
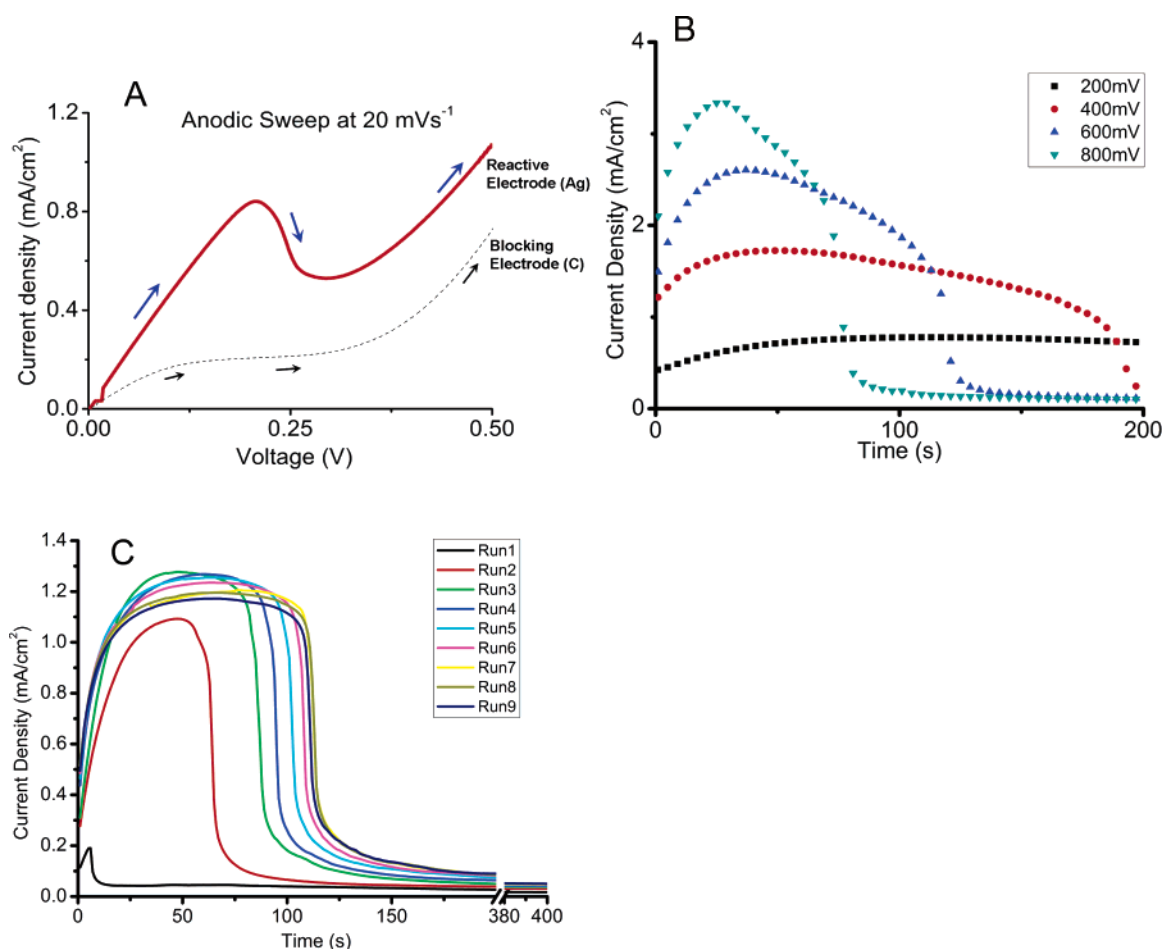
Figure 3. (A) Anodic sweeping of a Ag$_2$S stamp and reactive anode (Ag) or blocking (C) anode obtained at 20 mV/s provides clear evidence of ionic activity between 0.1 and 0.25 V. (B) Evolution of total current over etch time for the S4 stamping process run at 4 different applied bias with a silver sulfide stamp and silver substrate. The three (0.4, 0.6, and 0.8 V) that were run to completion show distinct phases of the processes from build up of ionic transport to a steady state, followed by a sharp decline as silver gets depleted at the anode. (C) Studies indicate potential of a very repeatable process. The current curves for nine repetitions of a stamping operation with a single new stamp at 0.3 V bias on 80 nm evaporated silver film substrate indicate convergence of the process to a steady-state repeatable current−time profile.

is interesting because the volume of silver dissolved in the different trials is nearly equal, but at a different potential level, the electronic current would be quite different. Taking the product of applied bias and the total charge transferred, and normalizing it by the amount of silver removed, our estimation shows a specific energy of 500 kJ/kg for the electrochemical imprinting of silver using a typical Ag$_2$S stamp. On the basis of the above observation, we can also estimate an average etch rate for an unpolarized (unused) silver stamp to be 1.28, 2.0, 3.16 nm/s for applied biases of 0.4, 0.6, and 0.8 V, respectively.

In addition, Figure 3C shows the temporal profile of etch current of a single stamp that has been stored for a few days prior to performing nine repetitions of the stamping process on different areas of an 80 nm thick silver film with a electrical bias of 0.3 V and a 30 s interval between each stamping. The same current profile as described previously is also observed for each repetition. Except for the first two runs, the total charge transferred is nearly constant. We have observed that the first two runs did not etch a complete pattern through the film and suspect that this is due to an oxidation layer formed on the silver sulfide stamp. Over the

nine repetitions of stamping, we have also observed the current profile to have evolved into having a slightly extended etching time and lower peak current as the current profile eventually settles down to a stable shape.

To demonstrate the fine resolution of the S4 process, in Figure 4, we performed an etching experiment with an amorphous silver layer coated onto borosilicate glass (samples from Arrandee). To obtain the 3D etch profile of the fine features from electrochemical imprinting, we conducted contact-mode atomic force microscopy (AFM) measurements on a Digital Instruments multimode system with an ultrasharp probe (20° tip angle, 10 nm tip radius) from MikroMasch. The samples were scanned with a scan area of 1 μm × 1 μm (corresponding to the dotted white lines in the upper panel) at a scan rate of 0.5 Hz. Both AFM and SEM measurements indicate that the smallest line width and spacing of 50 nm were transferred faithfully, reaching the resolution limit of the focused ion beam tool used for preparing the stamp. Also seen in the SEM micrograph in Figure 4 (top panel) is the apparent improvement in the surface roughness of the top surfaces of the pattern and the silver residue at the bottom. Such improved surface rough-
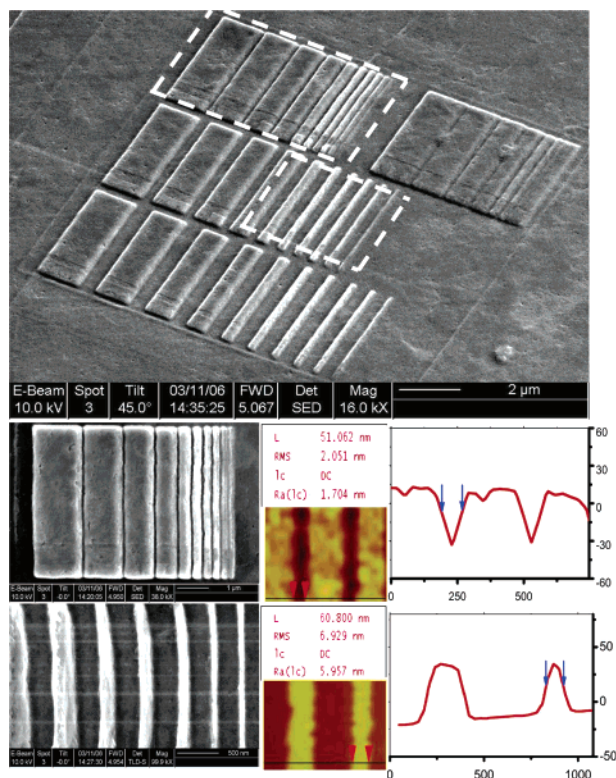
Figure 4. Demonstration of high-resolution transfer of channels and lines of varied width and spacing. (The line widths for all four sets of lines are 1600, 1200, 900, 600, 400, 250, 210, 170, 90, and 60 nm from left to right. The spacing is as follows: 50 nm for the line set on the top-left corner, 30 nm for the top-right set of lines by design but did not transfer onto the silver film, 200 nm for the center set, and 350 nm for the bottom set of lines. The feature height is around 100 nm for the thicker lines and reduces to 40 nm for the last two lines of width 90 and 60 nm.) Bottom panel: SEM and AFM of the fine trenches and ridges patterned onto silver film. The red curves are a cross-sectional profile of the AFM topographic images (bottom middle), showing 50 nm trenches are etched with at least 30 nm in depth, and 60 nm ridges, displaying a height of 50 nm.

ness is likely due to the nucleation-controlled anode dissolution at low overpotential conditions.

We also studied the process rates of a polarized stamp at steady state on a 470 nm silver film substrate (amorphous silver layer coated onto borosilicate glass, samples from Arrandee) with a driving potential of 0.3 V. Electrochemical etching or stamping was performed for different lengths of time, and the corresponding etch depths were measured using an AFM. As shown in Figure 5, the silver removal/etch rate throughout the process was found to remain constant at 4 nm/s. Remarkably, we obtained higher process rates than we had seen with new stamps on evaporated silver films. Further, a constant stamping rate implies constant ionic conductivity of silver sulfide in spite of the increase in silver concentration change or the composition change of the silver sulfide stamp. This is in good agreement with Hebb[15] and Wagner's[16] electrochemical measurements of β-phase silver sulfide (most stable at room temperature), which suggest that ionic conductivity of this phase is almost independent of composition within its stoichiometric range because the lattice structure of β-phase silver sulfide is quite open and
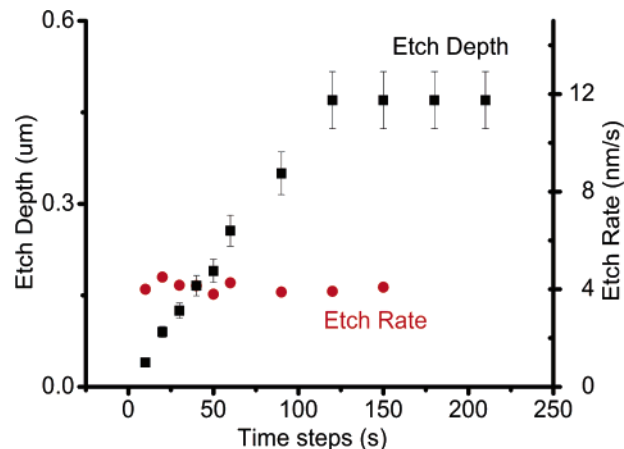
Figure 5. Steady-state etch rate for fully polarized Ag_2S stamp at applied bias of 0.3 V. The sample is a 470 nm thick silver film (amorphous silver film on borosilicate glass, samples from Arrandee). It indicates that, for a constant applied bias, the etch rate remains nearly constant and is independent of the depth to which the stamp has already traveled, facilitating the etching depth control.

is considerably rich in interstitial channels for motion and sites for residence of silver ions.

By assuming that the Ag_2S stamp was of ideal stoichiometry at the beginning of electrochemical reaction, we estimated the concentration of excessive silver absorbed into the stamp by calculating the amount of silver being oxidized and the affected volume of the stamp. The silver ion mass transport in the stamp is governed by the Nernst−Planck equation,[8] relating the transient concentration change to the chemical diffusion and electrochemical migration of the species in the stamp. For the time interval required to completely deplete the silver substrate, a characteristic diffusion layer thickness (proportional to the square root of the overpotential and the time wherein the bias was applied) is estimated to be around 500 μm. The total volume of silver removed was then calculated[17] to be approximately 4×10^{-11} m^3. As a result, at the end of one stamping operation, the local concentration of excessive silver ion in the diffusion-affected volume was estimated to change from 0 to 90 mol/m^3, or the stoichiometry ratio from 2 to 2.0017,[18] which is in the stoichiometric range of ionically conductive β-phase silver sulfide.

In conclusion, the S4 process offers a simple yet robust approach to manufacturing metallic nanostructures at 50 nm resolution. The process works under ambient conditions and does not require complex process steps or expensive equipment. The process rates and repeatability are surprisingly high (considering the rudimentary equipment and chemicals used and the fact that no process optimization was performed), and the S4 process can easily be scaled up for high-throughput production. Further, given the room-temperature operation, low voltages and highly localized nature of the transport phenomena exploited, we expect S4 to perform as an energy-efficient process. For the experiments reported here, the patterns were directly inscribed into the stamps using focused ion-beam milling. However, given the good ductility of silver sulfide, stamp patterns could readily be

produced by embossing with a hard master, leading to considerably more favorable process economics.

The exploitation of fast ionic conduction in solids as a manufacturing technique to produce high-resolution nanostructures, as exemplified by the S4 process, represents a new, efficient, and cost-effective avenue for current processes. While this letter has described patterning in silver with silver sulfide stamps, the process is not restricted to these materials. We have successfully patterned copper with similar results and consistency. For patterning metal structures, we will explore a variety of other ionic conductors such as Na^+, Cu^{2+}, and Pb^{2+} superionic conductors, solid polymer electrolytes, and glasses.

References

(1) Madou, M. *Fundamentals of Microfabrication*, 2nd ed.; CRC Press: New York, 2002.
(2) Ruska, W. S. *Microelectronic Processing*; McGraw-Hill: New York, 1987.
(3) Chou, S. Y.; Krauss, P. R.; Renstrom, P. J. *J. Vac. Sci. Technol., B* **1997**, *14*, 4129−4133.
(4) Chou, S. Y.; Krauss, P. R.; Zhang, W.; Guo, L.; Zhuang, L. *J. Vac. Sci. Technol., B* **1997**, *15*, 2897−2904.
(5) Zankovych, S.; Hoffmann, T.; Seekamp, J.; Bruch, J.-U.; Sotomayor Torres, C. M. *Nanotechnology* **2001**, *12*, 91−95.
(6) Trimmer, A. L.; Hudson, J. L.; Kock, M.; Schuster, R. *Appl. Phys. Lett.* **2003**, *82*, 3327−3329.
(7) Bhattacharyya, B.; Doloi, B.; Sridhar, P. S. *J. Mater. Process. Technol.* **2001**, *113*, 301−305.
(8) Rickert, H. *Electrochemistry of Solids*; Springer-Verlag: New York, 1982.
(9) Schuster, R.; Kirchner, V.; Xia, X. H.; Bittner, A. M.; Ertl, G. *Phys. Rev. Lett.* **1998**, *80*, 5599−5602.
(10) Avouris, P.; Hertel, T.; Martel, R. *Appl. Phys. Lett.* **1997**, *71*, 285−287.
(11) Terabe, K.; Nakayama, T.; Hasegawa, T.; Aono, M. *Appl. Phys. Lett.* **2002**, *80*, 4009−4011.
(12) Terabe, K.; Nakayama, T.; Hasegawa, T.; Aono, M. *J. Appl. Phys.* **2002**, *91*, 10110−10114.
(13) Lee, M.; O'Hayre, R.; Prinze, F. B.; Gur, T. M. *Appl. Phys. Lett.* **2004**, *85*, 3552−3554.
(14) Armstrong, R. D.; Dickinson, T.; Willis, P. M. *Electroanal. Chem. Interface Electrochem.* **1974**, *57*, 231−241.
(15) Hebb, M. *J. Chem. Phys.* **1952**, *20*, 185−190.
(16) Wagner, C. *J. Chem. Phys.* **1953**, *21*, 1819−1827.
(17) Silver atomic mass: 107.87 g/mol; density: 10.49 g/cm^3. Callister, W. D. *Materials Science and Engineering: An Introduction*; Wiley: New York, 2002.
(18) Hans, R. *Electrochemistry of Solids*; Springer-Verlag: New York, 1982; pp 165−166.

NL062766O